

Article

Precambrian Basement and Late Paleoproterozoic to Mesoproterozoic Tectonic Evolution of the SW Yangtze Block, South China: Constraints from Zircon U–Pb Dating and Hf Isotopes

Wei Liu ^{1,2,*}, Xiaoyong Yang ^{1,*}, Shengyuan Shu ¹, Lei Liu ¹ and Sihua Yuan ³

¹ CAS Key Laboratory of Crust–Mantle Materials and Environments, University of Science and Technology of China, Hefei 230026, China; syshu@mail.ustc.edu.cn (S.S.); liu01@ustc.edu.cn (L.L.)

² Chengdu Center, China Geological Survey, Chengdu 610081, China

³ Department of Earthquake Science, Institute of Disaster Prevention, Langfang 065201, China; yuansihua@gmail.com

* Correspondence: cdcgs_liuwei@163.com (W.L.); xyyang@ustc.edu.cn (X.Y.)

Received: 27 May 2018; Accepted: 30 July 2018; Published: 3 August 2018



Abstract: Zircon U–Pb dating and Hf isotopic analyses are performed on clastic rocks, sedimentary tuff of the Dongchuan Group (DCG), and a diabase, which is an intrusive body from the base of DCG in the SW Yangtze Block. The results provide new constraints on the Precambrian basement and the Late Paleoproterozoic to Mesoproterozoic tectonic evolution of the SW Yangtze Block, South China. DCG has been divided into four formations from the bottom to the top: Yinmin, Luoxue, Heishan, and Qinglongshan. The Yinmin Formation, which represents the oldest rock unit of DCG, was intruded by a diabase dyke. The oldest zircon age of the clastic rocks from the Yinmin Formation is 3654 Ma, with $\epsilon_{\text{Hf}}(t)$ of -3.1 and a two-stage modeled age of 4081 Ma. Another zircon exhibits an age of 2406 Ma, with $\epsilon_{\text{Hf}}(t)$ of -20.1 and a two-stage modeled age of 4152 Ma. These data provide indirect evidence for the residues of the Hadean crustal nuclei in the Yangtze Block. In combination with the published data, the ages of detrital zircons from the Yinmin Formation yielded three peak ages: 1.84, 2.30 and 2.71 Ga. The peaks of 1.84 and 2.71 Ga are global in distribution, and they are best correlated to the collisional accretion of cratons in North America. Moreover, the peak of 1.84 Ga coincides with the convergence of the global Columbia supercontinent. The youngest age of the detrital zircon from the Yinmin Formation was 1710 Ma; the age of the intrusive diabase was 1689 ± 34 Ma, whereas the weighted average age of the sedimentary tuff from the Heishan Formation was 1414 ± 25 Ma. It was presumed that the depositional age for DCG was 1.71–1.41 Ga, which was in accordance with the timing of the breakup of the Columbia supercontinent. At ~ 1.7 Ga, the geochemical data of the diabase were characterized by E-MORB and the region developed the same period A-type granites. Thus, 1.7 Ga should represent the time of the initial breakup of the Yangtze Block. Furthermore, the Yangtze Block continues to stretch and breakup until ~ 1.4 Ga, which is characterized by the emergence of oceanic island, deep-sea siliceous rock and flysch, representing the final breakup. In brief, the tectonic evolution of the Yangtze Block during the Late Paleoproterozoic to Mesoproterozoic coincided with the events caused by the convergence and breakup of the Columbia supercontinent, because of which, the Yangtze Block experienced extensive magmatic activity and sedimentary basin development during this period.

Keywords: Precambrian; Proterozoic; breakup; Dongchuan Group; Columbia supercontinent; Yangtze Block

1. Introduction

Among the Archean rocks that are extensively exposed in the Liaoning–Hebei–Henan area of the North China craton, many are reported to be as old as 3.8 Ga [1–5]. However, Archean rocks in the Kongling Complex are only exposed in a small area on the northern margin of the Yangtze Block [6–9]. Archean ages have also been reported from elsewhere on the Yangtze Block. For example, the captured zircons with ages of 2.5–2.6 Ga and 2.8–2.9 Ga have been observed in lamprophyre from Jingshan county, Hubei Province; Ningxiang county, Hunan Province; and Zhenyuan county, Guizhou Province [10]. An Archean age of ~2914–2955 Ma was established from the bentonite of the Meishucun Formation from the base of the Cambrian in Kunming, Yunnan Province [11]. An inherited zircon with an age of 2.7–2.8 Ga was observed in syenite from the Panxi area [12]. Detrital zircon as old as 3.8 Ga [13] exists, which is older than those of the Kongling Group. However, the ages of Archean rocks located in the western margin of the Yangtze Block have not been previously reported. The Kangding Group (or Kangding Complex) was previously considered to be the oldest crystalline basement on the western edge of the Yangtze Block [14,15]. However, recently, an increasing amount of research has reported the Kangding Complex to be a multi-stage deformed granite intrusion. It was formed in the Neoproterozoic rather, not in the previously recognized Archean–Paleoproterozoic [16–19]. Therefore, currently, it is not quite clear whether the Archean basement of the Yangtze Block is distributed only along the northern margin of the Yangtze Block or throughout the Yangtze Block.

The Yangtze Block is considered to preserve an important geologic record of the Late Paleoproterozoic–Mesoproterozoic convergence and breakup of the Columbia supercontinent [20–34]. In particular, the area between the western margin of the Yangtze Block (from the north of Kangding, Sichuan Province), the Yuanjiang county, the Yunnan Province to the south, the Puduhe Fault to the east, and the Yuanmou–Luzhijiang Fault to the west contains the most extensive distribution of the Paleoproterozoic to Proterozoic rocks in southern China. This area is ideal to study the Precambrian rocks of the Yangtze Block, especially the Paleoproterozoic–Mesoproterozoic geology. Various types of magmatic rocks are located on the western margin of the Yangtze Block, e.g., Late Paleoproterozoic–Mesoproterozoic ultrabasic to acidic rocks [27,35–40], and Paleoproterozoic–Mesoproterozoic sedimentary rocks, e.g., the Hekou Group, Dahongshan Group, and Dongchuan Group (DCG) [22,28,29,41–46]. Recently, the study of these rocks has generated considerable amount of geochronological and geochemical data. However, there are two different viewpoints on the depositional age of DCG in 1.8–1.5 Ga [19] and 1.7–1.5 Ga [28]. Moreover, the Late Palaeoproterozoic and Mesoproterozoic tectonic settings of this margin are not well defined. Currently, the interpretations range from an island-arc system related to the subduction that occurred 1.7–1.6 billion years ago [45,46] to a Late Paleoproterozoic–Mesoproterozoic plate-rift environment [22,28,29,31,42]. These different viewpoints constrain the understanding of the Late Paleoproterozoic–Mesoproterozoic tectonic setting of the Yangtze Block. Furthermore, because the Yangtze Block is a part of the Columbia supercontinent, research concerning the Paleoproterozoic–Mesoproterozoic tectonic evolution of the Yangtze Block provides data for the studying of the evolution of the Columbia supercontinent.

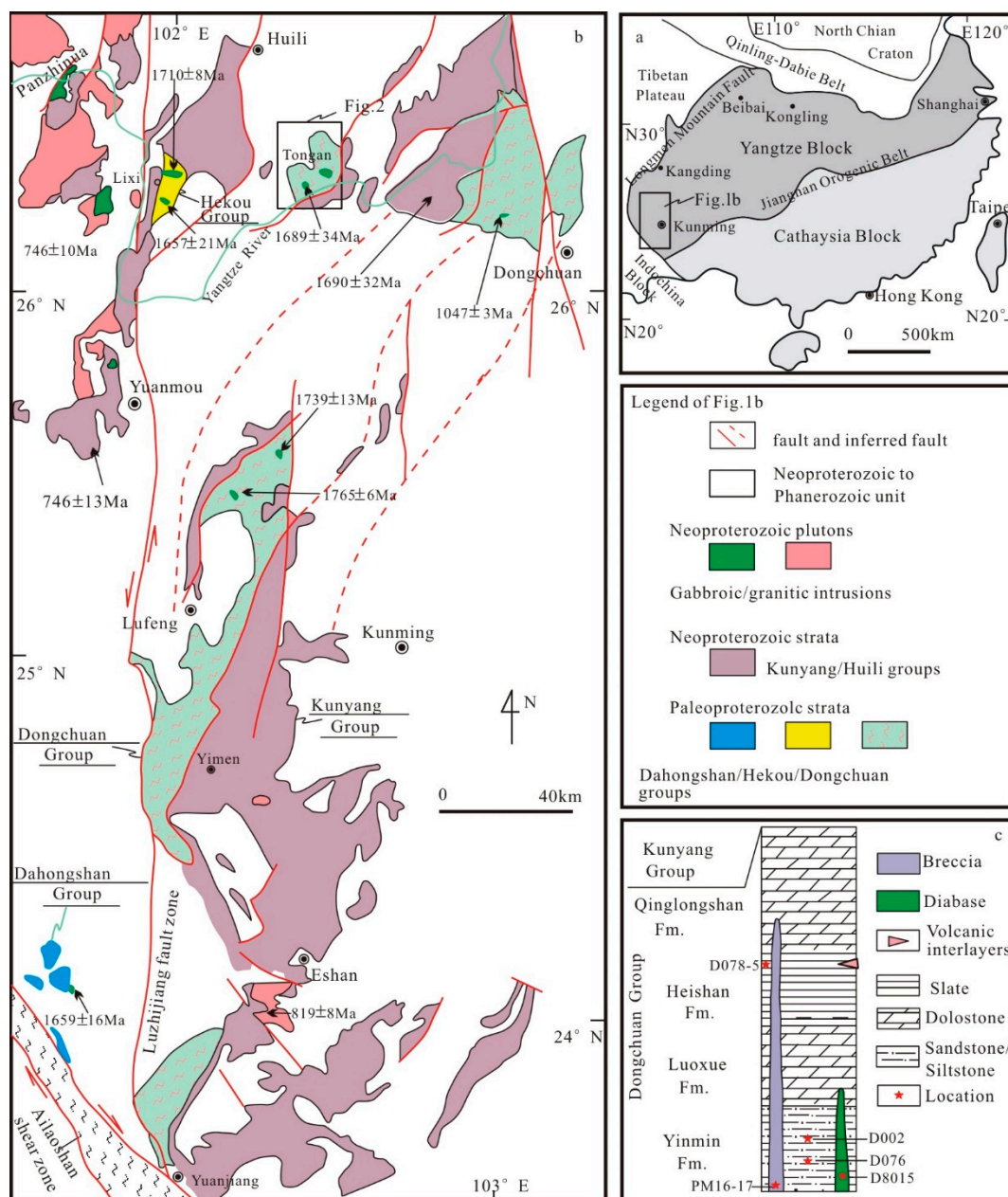
DCG is a typical representative of late Paleozoic to Mesoproterozoic deposits in SW of the Yangtze Block. Further, the DCG contains a large amount of geologic information from an era prior to the Mesoproterozoic. Therefore, the DCG can be regarded as an ideal unite for studying the growth and evolution of Proterozoic and Archean crustal of the Yangtze Block. Zircons have a strong ability to resist weathering. Even the oldest crust may retain some zircons after multiple events at later stages, which provides a possibility for comprehensive and accurate understanding of geological event sequences in specific areas. The content of Hf in zircons is high. Due to its high Hf content, the zircon Hf isotope system is highly stable and can retain its initial Hf isotopic information after multiple geological events. The zircon Hf isotope tracer is increasingly used widely for studying the growth and evolution of the oldest Earth's crust. This study discusses the Archean basement of the

Yangtze Block based on the zircon chronology and Hf isotopes of the clastic rocks from the Yinmin Formation, DCG. Combined with recent research results from this area, the tectonic evolution of SW Yangtze Block during the Late Paleoproterozoic–Mesoproterozoic and its relation with the evolution of the Columbia supercontinent are discussed.

2. Geological Background

The northwest of the Yangtze Block and Songpan-Ganzi Terrane on the eastern edge of the Tibetan Plateau are divided by the Longmen Mountain Fault. In the north, the Yangtze Block merged with North China during the Triassic Qinling–Dabie–Sulu orogeny [47,48]. Along the Ailao Shan–Red River fault, the southwest side of the Yangtze Block lies adjacent to the Indochina Block. The southeastern side of the Yangtze Block and the Cathaysia Block formed the present South China Block during the Neoproterozoic along the Jiangnan Orogenic Belt [49] (Figure 1a). Compared with North China, the Yangtze Block is characterized by extensive development of Neoproterozoic magmatic rocks, rather than by rocks that record the Archean to Paleoproterozoic geology. The Neoproterozoic magmatic rocks are extensively distributed on the periphery of the Yangtze Block and dominated by intermediate acid intrusive rocks and eruptive rocks, whereas basaltic rocks are observed in relatively few outcrops [50–55]. The Archean geology in the Yangtze Block is only exposed in the Kongling and Yichang areas on the northern margin of the Yangtze Block. The Yangtze Block also contains sedimentary records from the Paleoproterozoic–Cenozoic eras. The Mesoproterozoic–Triassic strata are dominated by the marine sediments, whereas most of the Upper Jurassic and younger strata are terrestrial sediments [56].

The western margin of the Yangtze Block, known as the Xikang–Yunnan axis, which is oriented in the north–south direction through Kangding, Xichang, and Yimen, is one of the most developed Precambrian areas in southern China. It has undergone multiple tectonic episodes since the Palaeoproterozoic, including the Dongchuan, Manyingou, Jinning and Yanshanian tectonic phases. In the Middle Proterozoic (c. 1400 Ma), the Dongchuan tectonic phase was dominated by north–south compression, forming E–W trending folds and fracture systems. The c. 1000 Ma Manyingou event formed several large north–south trending faults, including the Luzhijiang fault, the Puduhe fault, the Xiaojiang fault and the Anninghe fault. During the Jinning tectonic event at c. 820 Ma, massive ultrabasic–intermediate magma emplacement occurred, which was associated with NE trending open folds. The study area was generally tectonically quiescent during the Palaeozoic. Since the late Triassic, region has changed tectonic regime and was strongly influenced by tectonic activity in the Songpan–Ganze terrane to the west [14,15]. Magmatic rocks are dominated by the Mesoproterozoic basic and ultrabasic intrusive rocks, Neoproterozoic granites, and Permian Emeishan basalts. The Paleoproterozoic–Mesoproterozoic strata in the region mainly include the Kunyang, Tangdan, Hekou, Dahongshan, Dongchuan, and Huili groups and their metamorphosed equivalents (Figure 1b,c and Figure 2). The main lithologies are slate, phyllite, metamorphic sandstone, metamorphic volcanic rock, dolomite, and marble. All rocks have undergone varying degrees of metamorphism and deformation. The metamorphism of the SW Yangtze Block is mainly regional metamorphism, which is distributed in the pre-Ediacaran strata. The Ediacara and the younger strata did not experience regional metamorphism. The metamorphic rocks in this area include the Huili Group, Yanbian Group, DCG, Hekou Group, and Dahongshan Group. They have undergone one phase of greenschist facies metamorphism and the main metamorphic mineral assemblage is comprised of sericite and chlorite. There exist few contact metamorphic rocks and dynamic metamorphic rocks, which are scattered in the outer contact zone and fault zones [14].



The limited distribution of Archean–Paleoproterozoic geologic entities developed in the Yangtze Block is only exposed in the Kongling and Yichang areas on the northern margin of the Yangtze Block. The base of the Yinmin Formation mainly comprises purplish-red glutenite with gravels of various sizes, which are mainly subrounded and distributed discontinuously throughout the area (Figure 3a). Overlying the Yinmin Formation is mainly a set of quartz sandstone and feldspar quartz with miscellaneous sandstone (Figure 3b). Regionally, the Yinmin Formation comprises either terrigenous-clay clastic rock or carbonate rock rich in terrigenous debris. Because of alluvial fan-like purplish-brown conglomeritic layers in the lower strata of the Yinmin Formation, it is considered to be a continental feature, indicating the existence of either older landmasses or denuded areas. The Yinmin Formation may represent the sedimentary record of an earlier rift [60]. In the Tongan area of the

Sichuan Province, the lithology of the Yinmin Formation includes purple and purplish-red sandy slate, sandstone, greenish dolomite, pyroclastic rocks, and multilayered magnetic (hematite) iron ore convex mirror with plant microfossils. It reaches a thickness of 200–500 m and is in conformable contact with overlying limestone of the Luoxue Formation. The base of the Yinmin Formation has not yet been reached. The Luoxue Formation comprises thick light-gray, gray, and pale-red layers of algae, algal dolomite (Figure 3c), siliceous dolomite, silty dolomite, and calcareous slate. The thickness of the Luoxue Formation widely varies from tens of meters to several hundred meters, and it is in conformable contact with the overlying Heishan Formation located below the Yinmin Formation. The Heishan Formation is a set of dark gray and black carbonaceous slate as well as silty slate containing multiple layers of sedimentary tuff (Figure 3d). The slate is thin-layered, with a single layer thickness of approximately 5–8 cm, has stable lateral extension, and exhibits a thickness of more than 1100 m. In the Heishan Formation, black carbonaceous slate with a thickness of approximately 20–30 m is layered with slight graphite mineralization. The Heishan Formation is in conformable contact with the underlying Luoxue Formation and the overlying Qinglongshan Formation. The lithology of the Qinglongshan Formation is dominated by grayish-black dolomite and limestone, layered with black slate or argillaceous limestone (Figure 3e) and is in conformable contact with the underlying Heishan Formation. The Qinglongshan Formation is unconformable with the upper strata Chengjiang Formation (Nhc) in the Tongan area of the Yangtze Block (Figure 3f).

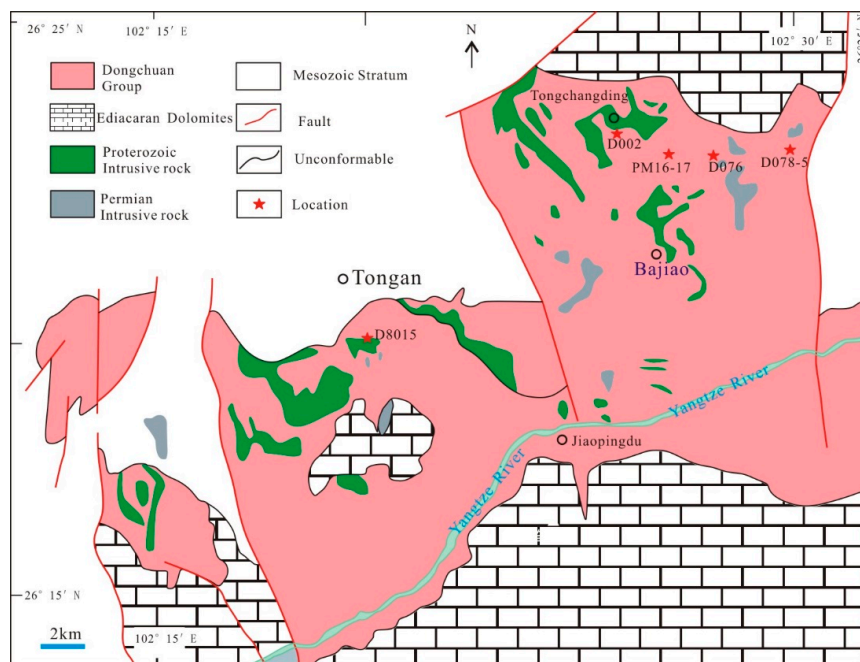


Figure 2. Simplified geological map of the study area (modified after paper [27]).

The bottom of the Yinmin Formation mainly comprises purplish-red glutenite, which is distributed intermittently in the area. It likely represents an alluvial fan-like environment. The central part of the upper of the Yinmin Formation is mainly comprises quartz sandstone and feldspar quartz heteroclast, which should be the product of the coastal shallow-water environment. Due to the evolution of the Yinmin period and the influence of the changes in the sea level in the Luoxue period, the sedimentary basin is dominated by a carbonate platform environment. In the Heishan period, the scope of the ancient land was greatly reduced. The Heishan Formation represents the deposition of shallow-to-deep-water basin and reflects the stability of basin development. In the Qinglongshan period, the sediments in the area have undergone major changes and have become a carbonate platform environment again.

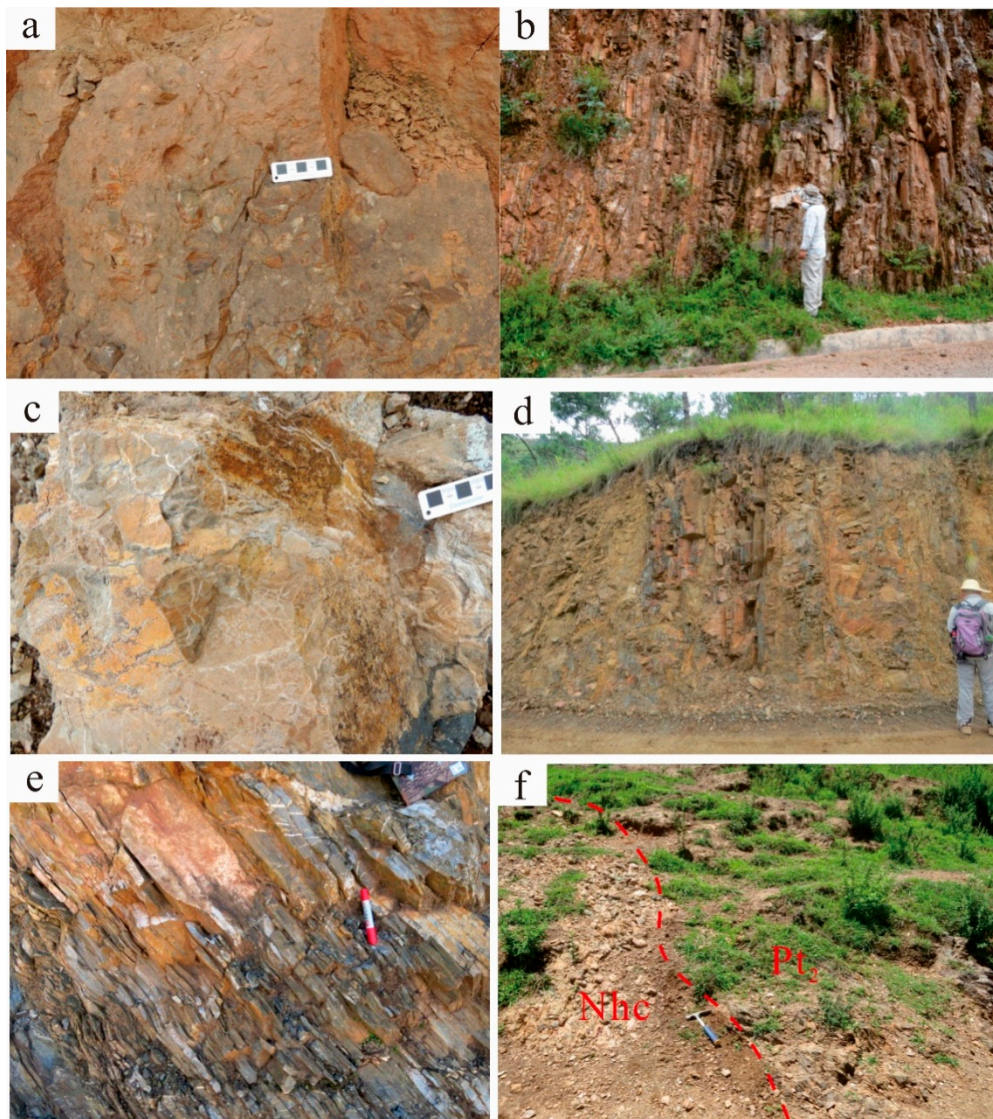


Figure 3. (a) Glutenite in the Yinmin Formation; (b) sandstone in the Yinmin Formation; (c) algal dolomite in the Luoxue Formation; (d) carbonaceous slate in the Heishan Formation; (e) dolomite and limestone in the Qinglongshan Formation; (f) unconformable contact between the Chengjiang Formation and the Qinglongshan Formation.

3. Sampling and Analytical Methods

One conglomerate (PM16-17) and two sandstones (D076 and D002) from the Yinmin Formation, one diabase (D8015) intruded into the Yinmin Formation, and one sedimentary tuff (D078-5) from the Heishan Formation, DCG, were sampled for this study. The petrography of the samples was examined, and zircons were selected for U–Pb dating. Hf isotopic analyses of some parts of the zircons were conducted. The locations of the studied samples are shown in Figure 2.

The conglomerate comprises of terrigenous clasts and interstitial fillings, and its geochemistry is not homogeneous. The components of the conglomerate are phyllite, andesite, and slate. We chose conglomerates in this study because they represent the oldest deposits of DCG. We chose different rocks at the bottom of DCG to ensure statistical significance. At the same time, we chose the sample to be as fine-grained as possible from the conglomerate. We also combined clast and matrix types. The terrigenous clastic debris, usually metasomatized by sodium feldspar, exhibits a sand-grain fabric; grain shapes are edge angle, hypo-edge angle, sub-rounded, and sometimes blurred (Figure 4a).

The size of the gravel is 2–7 mm, and the sand, ranging from 0.05–2 mm, is secondary. The gap between the interstitial material and the gravel is metasomatized by carbonate and albite. The terrigenous gravel comprises ~55% of the clasts, ~30% of sand and ~15% of the interstitial material. The vice minerals are opaque, and the secondary minerals are albite and carbonate.

Quartz sandstone comprises variable amounts of sand and interstitial material that is mainly composed of quartz with small amounts of feldspar and detritus (Figure 4b). The shape is mainly subrounded, and the circle is small. The particle sizes are grouped in the ranges 0.25–0.5 mm and 0.5–1.05 mm with a small amount of 0.1–0.25-mm-sized particles; they have a distressed mosaic-like fabric. The edges of the quartz grains exhibit secondary overgrowths. Feldspar is mainly streaked with small amounts of plagioclase and sericitization. The rock debris mainly comprises siliceous rock. The interstitial material comprises siliceous cement with small amounts of clay-based heterojunctions. The interstitial distribution is particle-supported, and the cementation is porous. The rock is locally fractured and filled with micro-quartz veins. The vein filling comprises >90% quartz, $\pm 5\%$ feldspar and debris, and <5% interstitial filling. A small amount of iron was observed filling the fractures. The sub-minerals are opaque tourmaline and zircon.

The diabase comprises phenocryst and a matrix. Phenocrysts comprise plagioclase with dark-colored mineral artifacts, have a particle size of 0.50–4.25 mm, and are distributed in a disorderly manner (Figure 4c). The plagioclases are subhedral plates with sericitization and carbonation. The dark-colored minerals, which are semi-angular, columnar-shaped, and resemble pyroxene artifacts, have been found to have altered to form aggregates of microscale-shaped flake chlorite and carbonate, with a small amount of limonite. The matrix comprises plagioclase and dark mineral artifacts, with a particle size of generally <0.4 mm. The plagioclases are subhedral slats, with a lattice-like distribution and dark mineral illusions distributed between them, forming a whitish-green structure with an alteration same as that of phenocrysts.

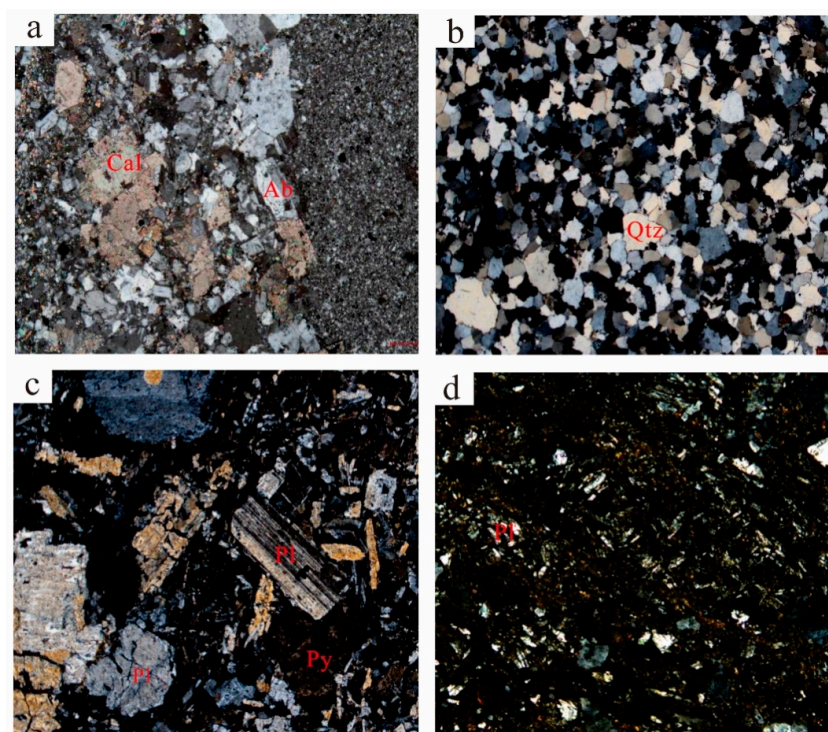


Figure 4. (a) Gravel structure, (+) 10×4 ; (b) medium coarse-grained quartz sandstone (+) 10×2 ; (c) porphyritic structure, (+) 10×2 ; and (d) tuff texture, (+) 10×5 (Ab = albite; Cal = calcite; Pl = plagioclase; Py = pyroxene; Qtz = quartz).

The sedimentary tuff sample is composed of tuff, rock detritus, and new metamorphic minerals (Figure 4d). The tuff particles are composed of lithic clasts, small amounts of crystals, glass shavings, and volcanic dust and the tuff fabric is mosaic-like and directional; this is partially explained by the presence of biotite. The rock detritus is mainly composed of rigid rock debris, which are irregularly shaped and are generally 0.4–1.2 mm in diameter, and mainly has an andesitic composition. The crystal fragments are composed of plagioclase and potassium feldspar with some quartz. They are subangular in shape and have a grain size of 0.2–1.3 mm. Some feldspar content retains a subhedral-plate shape. The vitric fragments and volcanic dust have been replaced by biotite. The unaltered sediments are composed of feldspar and detritus. They are subrounded and subangular. They are not distinguishable from the tuff and are partially metasomatized by biotite. The main components of the rock debris include andesitic. Feldspars include plagioclase and potassium feldspar.

Sorting of the zircons for dating was completed at the Langfang Regional Geological Survey Institute, Hebei Province. Using conventional magnetic separation and heavy liquid techniques to separate the zircon grains, the representative zircon grains were handpicked using a binocular microscope. The selected zircon grains were mounted in an epoxy resin and polished so that their diameters will become half their original diameter. Cathodoluminescence (CL) images were obtained using an electron probe microanalyzer (JXA-8100; JEOL Ltd.) at Beijing Geo Analysis Technology Co., Ltd., Beijing, China.

In situ U–Pb isotopic analyses of the zircons were performed using an LA–ICP–MS at the Chinese Academy of Sciences (CAS)–Key Laboratory of Crust–Mantle Materials and Environments, University of Science and Technology of China, Hefei, China. The analyses were conducted using ICP–MS (Agilent 7700 Quadrupole) coupled to a laser ablation system (Analyte HE 193-nm ArF Excimer; Teledyne Technologies Inc., Thousand Oaks, CA, USA) with a 6-Hz repetition rate and 60-mJ laser energy. The ablation spot diameter of the ion beam was set to 32 μm . Helium was applied as the carrier gas, and argon was used as the make-up gas. Each analysis comprised a background acquisition interval of approximately 20 s and a signal acquisition of approximately 40 s. The detailed parameters of the instrument can be found in a study by Liu et al. (2010) [61]. All the measurements were performed using zircon 91,500 as the external standard with a recommended $^{206}\text{Pb}/^{208}\text{U}$ age of 1065.4 ± 0.6 Ma [62] and were analyzed twice before and after every eight analyses. The raw data were first reduced using the ICPMSDataCal program [63] and then processed using the ISOPLOT program [64]. The individual analyses are presented with an error of 1σ in data tables and concordia diagrams; uncertainties in the age results are quoted at the 95% level (2σ).

In situ Lu–Hf isotopic analyses were conducted at the State Key Laboratory of Geological Processes and Mineral Resources. These analyses were conducted on the same zircons. The Lu–Hf isotopes were measured using MC–ICP–MS (Neptune Plus™, Thermo Fisher Scientific, Waltham, MA, USA), equipped with a 193-nm ArF-excimer laser ablation system. A spot size of 44 μm was used to perform the analyses with a laser repetition rate of 8 Hz at 100 mJ/pulse. Time-drift corrections and external calibration were performed using the zircon standard 91,500. Details of this analysis method and isotope fractionation correction are described by Wu et al. (2006) [65].

4. Results

4.1. LA–ICP–MS Zircon Dating

The ages of the samples in this study were all greater than 1000 Ma, and the ages used in the following discussion were all $^{207}\text{Pb}/^{206}\text{Pb}$ ages [66]. The concordance of the data used in our statistics is greater than 90%, and the error is less than 100 Ma. The results of U–Pb isotopic analyses are summarized in supplementary data Table S1.

The zircon CL images of the gravels (sample PM16-17) revealed that the zircons were mostly euhedral-subhedral granular in texture (Figure 5a). The zircons were mostly long-columnar, whereas some of the zircons exhibited obvious oscillating ring structures. The samples provided 86 valid

measurement points with Th/U values >0.1. The youngest zircon age was 1755 Ma while the oldest zircon age was 3497 Ma. There were three distinct age peaks of approximately 1.86, 2.28, and 2.70 Ga (Figure 5b).

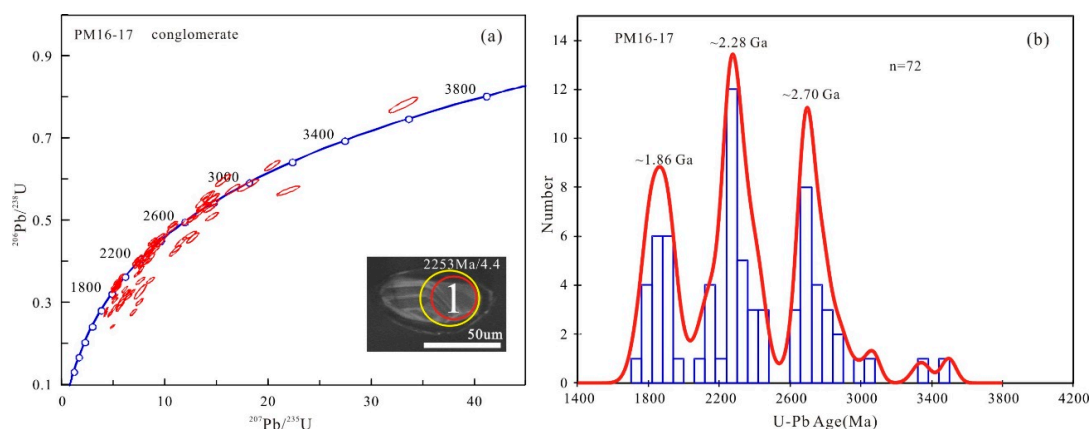


Figure 5. CL images and concordia plots (a) and statistical distribution (b) of zircon U–Pb dating for conglomerate (PM16-17) of DCG. Red and yellow circles indicate the locations of U–Pb dating and Hf analyses, respectively. U–Pb dating is undertaken first. This is also the case in Figures 6–9.

The CL images of sample D076 exhibited that the zircons were mostly self-shaped to semi-self-shaped and that some zircons were rounded, reflecting a significant modification through weathering and abrasion. Furthermore, certain parts of the zircons depicted core-edge structures (Figure 6a). The Th/U values of the 82 effective measurement points of the samples were all greater than 0.1. Only 19 points were observed to have values <0.4. On a concordia diagram of zircon (Figure 6a), some samples fell on the concordia line (Figure 6b). Some samples were near the concordia line, probably due to the old age. The zircons were affected by thermal events after their formation and were all older than 1700 Ma. The oldest zircon age was 3300 Ma, and the zircon ages showed three distinct peaks at 1.91, 2.34, and 2.62 Ga.

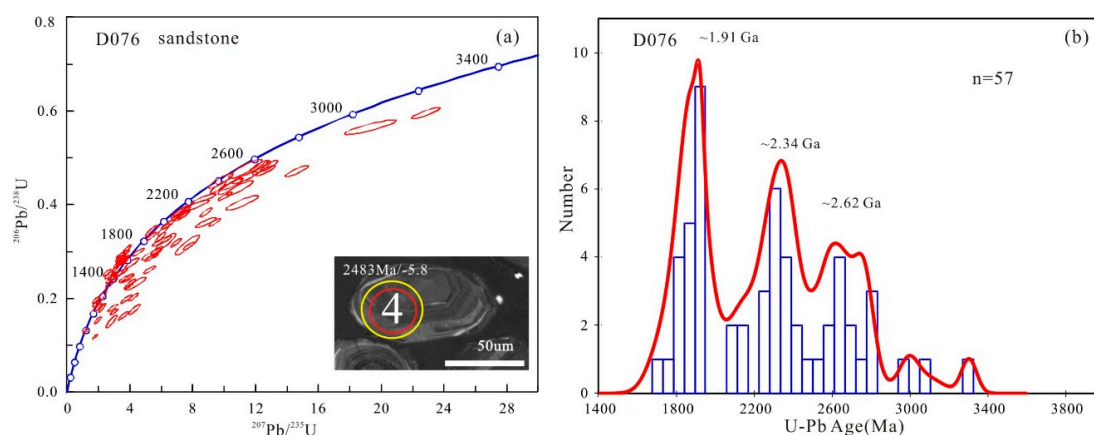


Figure 6. CL images and concordia plots (a) and statistical distribution (b) of zircon U–Pb dating for sandstone (D076) of DCG.

The zircons from sample D002 were mostly colorless and transparent, whereas some were brownish-red and light brown. Most zircons were distinctly rounded, reflecting some modification due to weathering or abrasion (Figure 7a). Some zircons were well preserved, which reflected a relatively small degree of transport and abrasion, presumably because they were located closer to their source area. Most zircons exhibited clear oscillatory zoning structures. The Th/U ratios of the 62 effective

measurement points were relatively high, except for one sample that depicted a ratio of 0.37. The ratios of all other measurement points were >0.4 , which reflected the magmatic origin of the zircons [67,68]. In the concordia diagram, most measured points deviated from the concordia line probably because the zircons were affected by the geologic events in a later period. Most of the zircon ages were concentrated in the range 2.0–3.0 Ga. The youngest was 1739 Ma, and the oldest was 3654 Ma among which three zircons were older than 3.0 Ga. There were two main peak and two sub-peak ages. The two main peak ages were ~ 1.90 and ~ 2.63 Ga (Figure 7b).

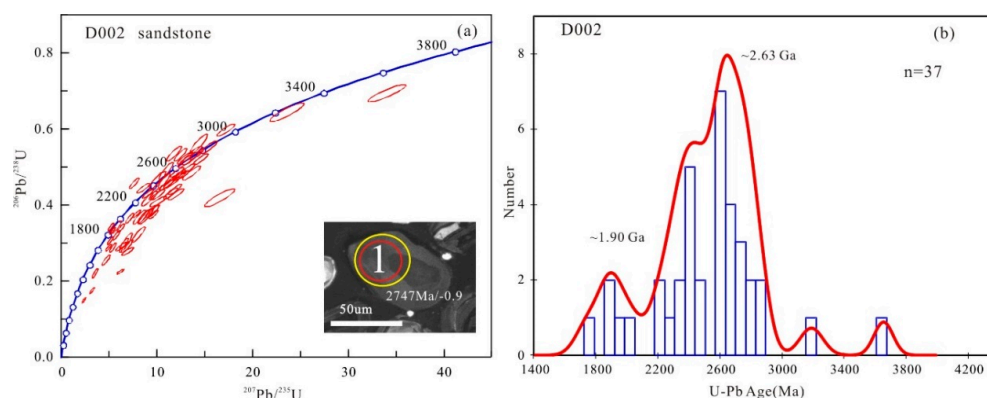


Figure 7. CL images and concordia plots (a) and statistical distribution (b) of zircon U–Pb dating for sandstone (D002) of DCG.

The zircons in sample D8015 were present in small quantities, were mostly light yellow, and had euhedral-subhedral granular shapes with no rounding. The CL images showed that the zircons were mostly euhedral–subhedral granular in texture with no obvious core–edge structures and mostly long columnar structures. A few zircons had oscillation ring structures. The Th/U ratios of the 20 effective measurement points were between 1.23 and 4.96, which reflected the magmatic origin of the zircons [67,68]. The 20 age points exhibited an age range of 1494 to 1794 Ma, which was relatively large. This may be due to a certain degree of influence from later tectonic thermal events. In the zircon U–Pb harmonic diagram, the point data deviated from the concordia line and fell on an inconsistent curve. The age of the upper intersection was 1689 ± 34 Ma (MSWD = 2.1), and this age would represent the intrusion of the diabase (Figure 9). It was depicted that the sedimentation start point of the population group should be greater than 1.7 Ga. This age is consistent with the extensively developed magmatic activity of approximately 1.7 Ga in the region.

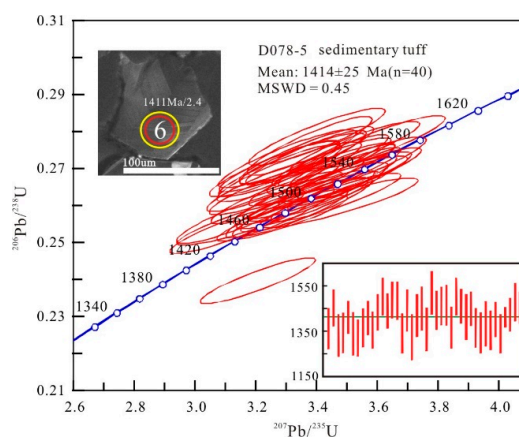


Figure 8. CL images and concordia plots of zircon U–Pb dating for the sedimentary tuff of Dongchuan (D078-5).

The zircons from sample D078-5 were mostly short columnar and plate-like with no obvious nucleus structures; clear oscillatory ring structures could be observed in some samples. They had no obvious characteristics from abrasion, indicating that did not undergo handling and redeposition. The Th/U values of the 40 effective zircon points were relatively high: all values were all greater than 0.4 and between 0.52 and 1.54. This is a typical zircon feature of the magmatic rocks. On the zircon U–Pb harmonic map, the measured data were distributed on or near the concordia line, and the ages were very consistent. The weighted average age was 1414 ± 25 Ma (MSWD = 0.45; Figure 8). This age represents the age of the magmatic event during this period.

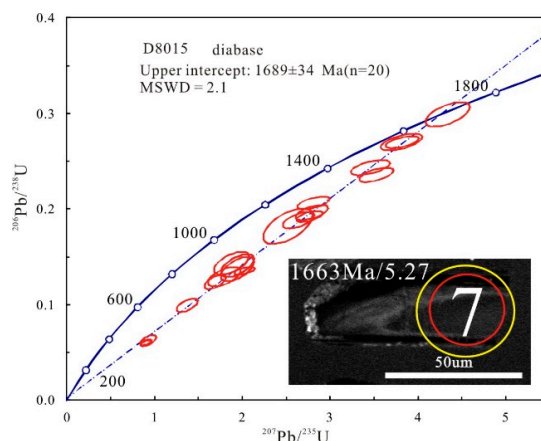


Figure 9. CL images and concordia plots of zircon U–Pb dating for diabase (D8015).

4.2. Zircon Lu–Hf Isotopic Compositions

To study the growth and evolution of the ancient crust in the Yangtze Block, Hf isotopic analyses were performed after the zircon U–Pb isotope measurement. The parameters used for the calculation of the Hf isotopic composition of the zircons were the ^{176}Lu decay constant $\lambda = 1.867 \times 10^{-11}$, chondrite $^{176}\text{Lu}/^{177}\text{Hf} = 0.0332$, $^{176}\text{Hf}/^{177}\text{Hf} = 0.282772$ [69], depleted mantle $^{176}\text{Lu}/^{177}\text{Hf} = 0.0384$, and $^{176}\text{Hf}/^{177}\text{Hf} = 0.28325$ [70]. The results of Lu–Hf isotopic analyses are listed in supplementary data Table S2.

Only a few zircon Hf isotope $\varepsilon_{\text{Hf}}(t)$ values from the three samples of the clastic rock were positive, and only one data point was located on the depleted mantle evolution line, whereas the other data points were below the depleted-mantle line. Therefore, a two-stage modeled age (T_{DMC}) was used to discuss the age of the crustal growth. Due to the complex source and dispersion ages of the Yinmin Formation, the apparent age was used to calculate the modeled age. For the intrusion of the diabase into the Yinmin Formation, the modeled age was calculated using the upper intersection point (1690 Ma). The zircon $\varepsilon_{\text{Hf}}(t)$ values were all positive and located near the mantle deficit line; therefore, only one stage of the modeled age is discussed. The sedimentary tuff (D078-5) collected from the Heishan Formation had more concentrated zircon ages, which represented the origin of a magmatic event. The modeled age was calculated using the weighted mean age. $\varepsilon_{\text{Hf}}(t)$ of the zircons was both positive and negative and below the mantle evolution line. Therefore, the two-stage modeled age was used to estimate the age of the crustal growth.

For the sampled zircons of the Yinmin Formation, there were 108 effective measurement points of the Hf isotopes. The $^{176}\text{Lu}/^{177}\text{Hf}$ ratio ranged from 0.000065 to 0.002967, whereas $^{176}\text{Hf}/^{177}\text{Hf}$ ratio ranged from 0.280385 to 0.281872. The $\varepsilon_{\text{Hf}}(t)$ values ranged from -20.1 to 9.1 , with 36 positive values and 72 negative values. The ratio of positive to negative values was 1:2. When $\varepsilon_{\text{Hf}}(t)$ was negative, the age of the two-stage model was significantly greater than the surface age, indicating that the material was derived from the remelting of the ancient crust. The $\varepsilon_{\text{Hf}}(t)$ value of the oldest zircon (3654 Ma) was -3.1 , and the two-stage modeled age reached 4081 Ma. Among all the measurement

points, there were 58 points in the two-stage modeled age that were older than 3000 Ma and the oldest reached 4152 Ma. These ages recorded the evolution of the Earth's early crust.

The zircon $\epsilon_{\text{Hf}}(t)$ values of the diabase were all positive and ranged from 3.4 to 11.9, with an average of 8.0. The age of the one-stage modeled T_{DM} was 1688–2007 Ma, and the upper intersection point was 1689 Ma. The material may have directly originated directly from the mantle (Figure 10). The $\epsilon_{\text{Hf}}(t)$ value of the zircon from the sedimentary tuff that was sampled from the Heishan Formation was both positive and negative and ranged from -4.1 to $+3.7$ with an average of 0.9. The age of the two-stage model was 1937–2419 Ma with an average of 2115 Ma (Figure 10).

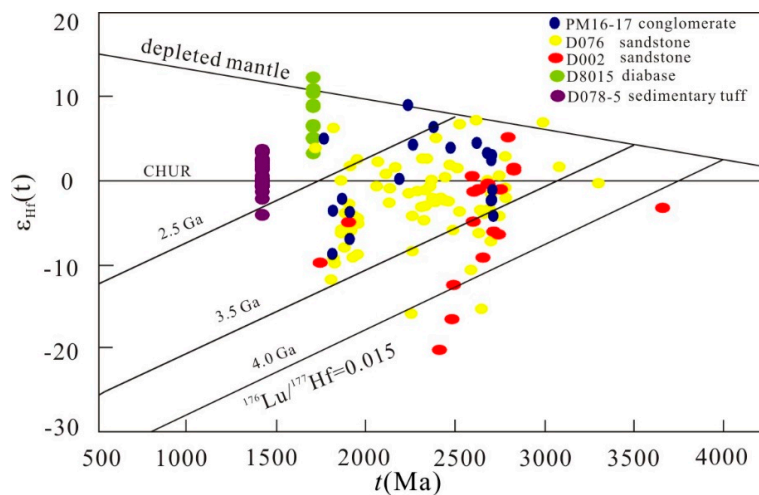


Figure 10. Hf isotope composition of zircons from DCG and a diabase in the western margin of the Yangtze Block.

5. Discussion

5.1. Ancient Geological Records and the Basement of the Yangtze Block

The early evolution of the solid crust is important to study Earth science, especially Early Precambrian geology. The study of the formation and evolution of the Precambrian continental crust is important to understand the continental dynamics and develop the theory of plate tectonics. The oldest crustal rocks that have been found to date are Acasta gneisses in the Wopmay orogenic belt of North America, Canada, which are formed in 4016 Ma [71]. The oldest known zircon on Earth is a detrital zircon from the Jack Hills and adjacent areas in the northern Yilgarn Craton, Western Australia with a $^{207}\text{Pb}/^{206}\text{Pb}$ age of 4404 ± 8 Ma [72]. The oldest rocks, comprising granite, felsic gneiss, and quartz diorite, are found in the Anshan area of North China and are aged 3.8 Ga [1–5]. This is also the oldest recorded rock found in China. The oldest rocks in North China are Anshan granites, felsic gneisses, and quartz diorites with an age of 3.8 Ga, which is the oldest record of rock found in China. The Tarim–North China plate is considered to contain extensively distributed Archeozoic–Paleoproterozoic basement. However, there are only a few Archean to Early Paleoproterozoic or older rocks that are exposed on the surface of the neighboring Yangtze Block. The surface Archean rocks that were reported from the Yangtze Block have only been exposed to the north of the Yangtze Block. These are ~ 2.9 – 3.3 Ga Kongling Complex rocks in the Kongling area [7,8,10]. The outcropping area of the Kongling Complex is ~ 360 km², mainly composed of ancient tonalitic granite diorite–trondhjemite–diorite (TTG), gneiss, migmatite, altered sedimentary rocks, and amphibolite with a small amount of granulite. According to the U–Pb age analyses of the zircons via LA–ICP–MS and SHRIMP, the TTG magmatism in the Kongling area mainly occurred around 2.85–2.95 Ga, and some occurred at around 3.2–3.3 Ga [8,73–75]. There exist multiple Archean–Early Proterozoic ages reported from other areas of the Yangtze Block. The Archean–Early Proterozoic ages

for zircons with inherited cores or upper intercepts were observed in the Huangtuling granulites [76] and Shuanghe eclogites [77,78] in the northern Dabie Mountains and the Wulian granitoids in the Sulu region [79]. Zircons with inherited nuclear ages of 2.69–2.82 Ga (using SHRIMP) are found in Triassic Maomaogou alkaline rocks [12] from the Western Panzhihua area, and 2.47-Ga-inherited nuclear zircon ages have been reported in the Neoproterozoic granitic gneiss from Shaba, Mianning County, Sichuan Province [80]. A large number of Archean to Early Proterozoic detrital zircons have also been found in sedimentary rocks deposited over different periods within the Yangtze Block. For example, in the Sanxia area, Hubei Province, Liu et al. (2005) discovered a large number of detrital zircons aged 3.3–3.5 Ga from Sinian sandstones and tillite [81]. Detrital zircons aged 2.63–2.47 Ga from the Cambrian and Ordovician sedimentary rocks have been observed by Zhang et al. (2016) to the north of Hunan and Guangxi [82]. Greentree and Li also discovered a large amount of ancient detrital zircons aged 2.5–3.0 Ga in metamorphic rocks from the Dahongshan Group, located on the southwestern margin of the Yangtze Block [83]. In addition, there are also small amounts of Archean strata exposed in the Song Da area of Vietnam [84,85]. For example, Lan et al. studied the age of gneiss in the Cavin Complex and observed that the zircon U–Pb age was 2.8–2.5 Ga, and the Nd modeled age was 3.4–3.1 Ga [85].

Herein, of the 230 valid measurement points in zircons obtained from the Yinmin Formation clastic rock, 10 points were older than 3.0 Ga and 82 points were dated between 2.5 and 3.0 Ga. One of the zircons that had an age of 2406 Ma had a zircon $\epsilon_{\text{Hf}}(t)$ value of -20.1 , and the two-stage modeled age reached 4152 Ma. Among all the measured points, the oldest zircon was 3654 Ma, with a $\epsilon_{\text{Hf}}(t)$ value of -3.1 and a two-stage modeled age of 4081 Ma. This modeled age is similar to the Hf modeled age of 3.8 Ga from a detrital zircon from the Yangtze Block reported by Zhang (2006) [13]. This may indicate that the Yangtze Block is older than the Kongling high-grade metamorphic rocks of the Archean crustal fragments from the Hadean.

The ages obtained from the Yinmin Formation, DCG, located on the western margin of the Yangtze Block were mainly in the range 1.7–3.0 Ga. At ~ 2.95 Ga, the frequency of age data increased significantly, indicating that magmatic activity was significantly enhanced. The magmatic activity was enhanced 2.95 Ga ago (Figure 11), which is consistent with the time range of the ~ 2.85 – 2.95 Ga magmatism from the northern margin of the Kongling Complex, indicating that a large area of the Yangtze Block preserves a geological record that depicts an age similar to that of the Kongling Complex. Further, $\epsilon_{\text{Hf}}(t)$ was mostly negative and the two-stage modeled age was between 2.5 and 4.0 Ga. This indicated that the early-stage crustal matter may have been differentiated from the mantle during the early Archean.

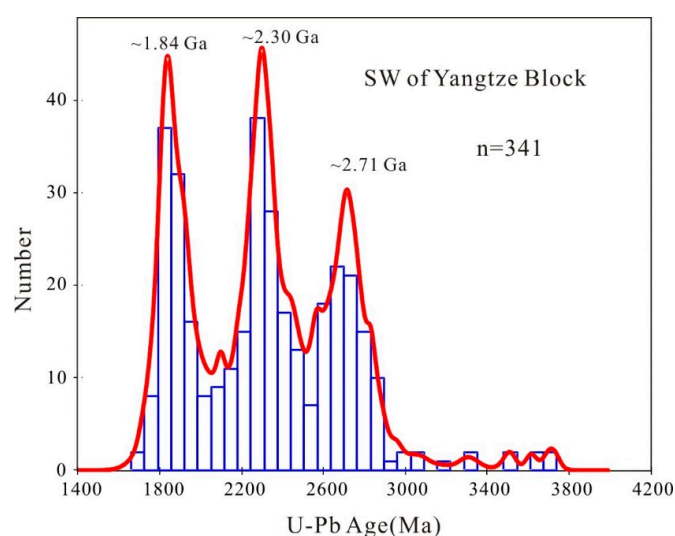


Figure 11. Histogram of compiled concordant detrital zircon U–Pb ages > 1700 Ma in the SW Yangtze Block. Data are from [22,28] and the present study.

In combination with published data, the ages of detrital zircons from the Yinmin Formation yielded three peak ages of 1.84, 2.30 and 2.71 Ga (Figure 11). These data revealed three important global geological events. The first event coincides with the convergence of the global Columbia supercontinent. The peaks of 1.84 and 2.71 Ga are distributed globally, and they are best correlated to the collisional accretion of cratons in North America [86] (Figure 12). The 2.1–1.8-Ga orogens have been recognized on nearly every continent, including the Eburnean Orogen of West Africa, the Transamazonian Orogen of South America, the Svecofennian and Kola–Karelia Orogens of northern Europe, the Trans-Hudson Orogen and its age-equivalent orogens of North America, the Capricorn Orogen of Western Australia, the Akitan and Central Aldan Orogens of Siberia, the Transantarctic Mountains Orogen of Antarctica, and the Trans-North China Orogen in North China [87].

5.2. Late Paleoproterozoic Tectonic Evolution of the Yangtze Block and Columbia Supercontinent Convergence

The Columbia supercontinent comprised three continental block groups: Ur, Nena, and Atlantica (Atlantic). During the Paleoproterozoic (~2.0–1.8 Ga), these continental blocks gradually converged to form a supercontinent [21,86,88,89]. The age obtained from the Yinmin Formation depicts that the 2.0–1.8 Ga magmatism was also widely developed on the western margin of the Yangtze Block, with a significant peak age of ~1.85 Ga. Paleoproterozoic (~2.0–1.8 Ga) metamorphic–magmatic activities were recorded across the whole Yangtze Block. Zhang et al. (2006) determined that the Paleoproterozoic (2.0–1.8 Ga) metamorphic magmatism was developed in the Northern Yangtze Block by analyzing the U–Pb age and Hf–O isotopes of zircons from argillaceous rocks and amphibolites in the Kong Ling area [90], which is in accordance with the viewpoint of Wu et al. (2009) [75]. Zhang et al. (2006) also reported the same metamorphic age for migmatites in Yemadong, Hubei Province [90]. Ling Wenli et al. (2001) obtained a metamorphic age of ~1.95 Ga by analyzing the whole rock Sm–Nd isotopes of the Kongling amphibolites and plagiogneisses [91]. In addition, the 1.85 Ga intrusions of moyite [92] and 1.97–2.03 Ga granites as well as basic dykes were also found in the northern part of the Yangtze Block [93]. The ages of the granite and basic-rock walls are younger than that depicted by metamorphism, which is generally considered to be the result of post-orogenic cracking [93].

These ages (~2.0–1.8 Ga) in the Yangtze Block are mainly distributed in the north (Kongling and Jingshan), south (Yiyang and Ningxiang), southwest (Longsheng and Kunming), east (Maanshan), and Dabie and Sulu orogenic belts. These manifestations of zircon can be divided into three types: (1) high-grade metamorphic zircons or accretionary margins, (2) captured zircons, and (3) inherited zircons. Tectonic thermal events during the 2.0–1.8 Ga period are widespread in the North China plate and are globally developed during the convergence of Columbia.

The 2.0–1.8 Ga magmatic activity in the Yangtze Block is widely developed and is observed to occur during the convergence of Columbia [21,94] (Figure 12). Therefore, this magmatic activity may have a genetic relation with Columbia, resulting from its convergence.

5.3. Late Paleoproterozoic–Mesoproterozoic Tectonic Evolution of the Yangtze Block and the Breakup of the Columbia Supercontinent

At around 1.85 Ga, the tectonic setting of the Yangtze Block dramatically changed after the arc-continent collision convergence stage during the 2.0–1.8 Ga-interval. A-type granite and basal veins that were aged 1.85 Ga were developed in the Kongling area of the Yangtze Block [93], and A-type acid rocks of ~1.87–1.82 Ga were developed in the Huashanguan area of Zhongxiang [94]. They were formed in a post-orogenic or post-collision tectonic environment. Simultaneously, at ~1.79 Ga, A-type granites were developed in the Beiba area of the Yangtze Block. In the Nb–Y–Ce diagram proposed by Eby et al. (1992) [95], they were all categorized as A2-type granites in post-collision and/or post-orogenic environments [33]. This indicates that any structural transformation, including collision and extension, occurred during the Late Paleoproterozoic in the Yangtze Block.

Herein, 187 effective measuring points were obtained from the clastic rocks of the Yinmin Formation from the base of DCG with zircon U–Pb ages between 1710 and 3654 Ma. The age

of the upper intersection of diabase that intruded into the Yinmin Formation was 1689 ± 34 Ma, which indicated that the sedimentary age of the Yinmin Formation was earlier than the magmatic event. From the zircon U–Pb dating of the sedimentary tuff (D078-5) from the upper part of the Heishan Formation, DCG, we observed that the weighted average age was 1414 ± 25 Ma. Therefore, the depositional age of the DCG should be between 1.7 and 1.4 Ga, which was in accordance with the timing of the breakup of the Columbia supercontinent.

The age of the diabase is 1689 ± 34 Ma (MSWD = 2.1) in this study, which is consistent with the results for the ages 1694 ± 16 Ma [27] and 1692 ± 32 Ma [22] in the error range of the previous studies, indicating that there is a significant magmatic activity in the SW Yangtze Block in 1.70 Ga. The $\epsilon_{\text{Hf}}(t)$ value of the diabase is mostly positive, the one-stage model age is similar to the zircon age, and the geochemical data are characterized by E-MORB [27], indicating that the material source may directly originate from the enriched mantle. Simultaneously, a 1.73 Ga A-type Haizi granite porphyry is developed in the area [37]. This information indicates that the Yangtze Block began to rift at 1.7 Ga (Figure 12). Meanwhile, the lower part of the DCG comprises either terrigenous clastic rocks or a rich source of detrital carbonate. In addition, purple sandstone and alluvial-fan facies found in the lower strata of the Yinmin Formation indicate the existence of an older continent or erosional area. The marginal facies sediments, found in the Lixi Zhongchang section, comprise sandstone and mudstone assemblages from the coastal and shallow-sea environments. Simultaneously, in the area of Dongchuan, accumulation of tidal flat estuarine facies constitutes a marginal phase unit, indicating the existence of an ancient landmass or denudation area. This indicates that most of the research area during the Yinmin Formation period was likely to have been eroded [60]. This may represent a sedimentary formation in an early rift feature.

The Yangtze Block begins to rift at ~ 1.7 Ga and continues to extend. Until about 1.4 Ga, the Tongan area development—a double-layered stratum with oceanic volcanic bases and carbonate cap rocks and its rock composition sequence were consistent with those of oceanic islands or seamounts. The spider diagram of the trace element ratio and the REE distribution patterns of volcanic rocks show the characteristics of OIB (Table S3). Moreover, deep-sea siliceous rocks and flysch of the same period are preserved in the Tongan area. These results indicate the breakup of the Yangtze Block into the opening ocean (Tongan ocean), with an oceanic island at ~ 1.4 Ga.

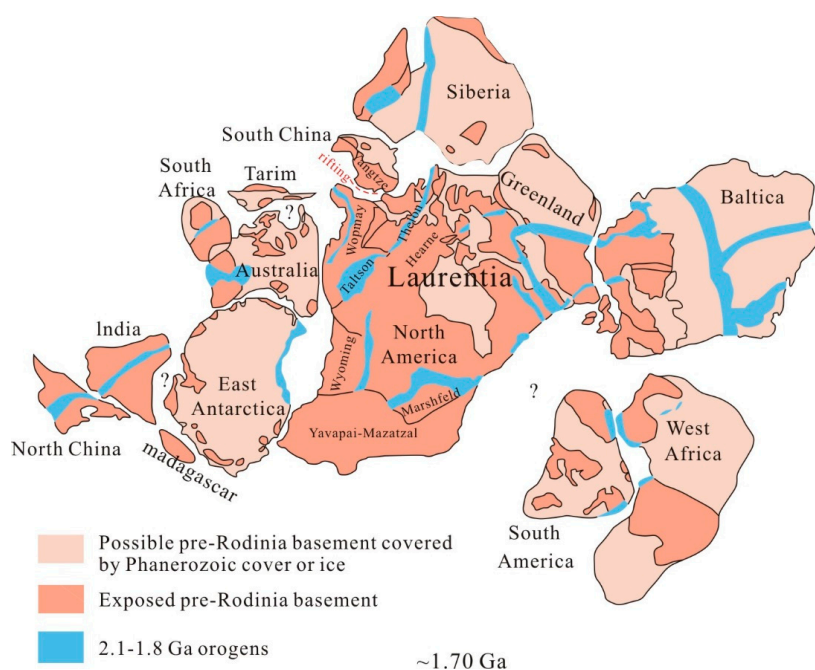


Figure 12. Reconstruction of the proposed Columbia supercontinent (modified after paper [21]).

In summary, the magmatic activity and sedimentary basin formed during the ~2.0–1.4 Ga period, which were widely developed in the SW Yangtze Block, and coincided with the events caused by the convergence and breakup of the Columbia supercontinent. It is proposed that the Yangtze Block was part of the Columbia supercontinent during the Paleoproterozoic to Mesoproterozoic. The magmatic activity and the sedimentary basins in this period are related to the evolution of the Columbia supercontinent.

6. Conclusions

- (1) The oldest basement rocks in the Yangtze Block were aged between 2.85 and 2.95 Ga, equivalent to the age of the Kongling Complex. The Yangtze Block preserved information about the residues of the crustal nuclei during the Hadean.
- (2) The ages of detrital zircons from the Yinmin Formation yielded three peak ages of 1.84, 2.30 and 2.71 Ga. The peaks of 1.84 and 2.71 Ga are globally distributed, and they are best correlated to the collisional accretion of the cratons in North America. Moreover, the peak of 1.84 Ga coincides with the convergence of the global Columbia supercontinent period.
- (3) The depositional age of DCG was ~1.7–1.4 Ga. DCG was a geologic record of the extension and breakup during the Late Paleoproterozoic–Mesoproterozoic.
- (4) Some parts of the Columbia supercontinent probably began to breakup in 1.7 Ga. The Yangtze Block breakup eventually occurred from the Columbia supercontinent at ~1.4 Ga.

Supplementary Materials: The following are available online at <http://www.mdpi.com/2075-163X/8/8/333/s1>. Table S1: LA–ICP–MS zircon U–Th–Pb analysis data of DCG and a diabase in the SW Yangtze Block. Table S2: Lu–Hf isotopic data for the zircons of DCG and a diabase in the SW Yangtze Block. Table S3: Whole-rock analyses of major elements (wt %), and trace elements (ppm) of the Mesoproterozoic sedimentary tuff in the SW Yangtze Block.

Author Contributions: W.L. was the chief investigator of the project and constructed the manuscript; X.Y. conducted discussions and manuscript editing; S.S. conducted optical microscopic observation; L.L. conducted the LA–ICP–MS analysis and data interpretation; S.Y. performed the figure/diagram production and discussion.

Acknowledgments: This study was financially supported by the National Key R&D Program of China (No. 2016YFC0600404), the National Natural Science Foundation of China (Nos. 41673040, 41773026, and 41772200), and fund for the geological survey from the Ministry of natural resources of PRC (Nos. DD20160016 and DD20160017). The authors would like to thank Enago (www.enago.cn) for the English language review. Constructive and critical comments by two anonymous reviewers result in the significant improvement of the manuscript.

Conflicts of Interest: The authors declare no conflict of interest.

References

1. Song, B.; Nutman, A.P.; Liu, D.; Wu, J. 3800 to 2500 Ma crustal evolution in the Anshan area of Liaoning Province, northeastern China. *Precambrian Res.* **1996**, *78*, 79–94. [[CrossRef](#)]
2. Wan, Y.; Liu, D.; Song, B.; Wu, J.; Yang, C.; Zhang, Z.; Geng, Y. Geochemical and Nd isotopic compositions of 3.8 Ga meta-quartz dioritic and trondhjemitic rocks from the Anshan area and their geological significance. *J. Asian Earth Sci.* **2005**, *24*, 563–575. [[CrossRef](#)]
3. Wu, F.; Zhang, Y.; Yang, J.; Xie, L.; Yang, Y. Zircon U–Pb and Hf isotopic constraints on the Early Archean crustal evolution in Anshan of the North China craton. *Precambrian Res.* **2008**, *167*, 339–362. [[CrossRef](#)]
4. Zhai, M.; Santosh, M. The Early Precambrian odyssey of the North China craton: A synoptic overview. *Gondwana Res.* **2011**, *20*, 6–25. [[CrossRef](#)]
5. Zhao, G.; Zhai, M. Lithotectonic elements of precambrian basement in the north china craton: Review and tectonic implications. *Gondwana Res.* **2013**, *23*, 1207–1240. [[CrossRef](#)]
6. Gao, S.; Ling, W.; Qiu, Y.; Lian, Z.; Hartmann, G.; Simon, K. Contrasting geochemical and Sm–Nd isotopic compositions of Archean metasediments from the Kongling high-grade terrain of the Yangtze craton: Evidence for cratonic evolution and redistribution of REE during crustal anatexis. *Geochim. Cosmochim. Acta* **1999**, *63*, 2071–2088. [[CrossRef](#)]

7. Zhang, S.; Zheng, Y.; Wu, Y.; Zhao, Z.; Gao, S.; Wu, F. Zircon isotope evidence for ≥ 3.5 Ga continental crust in the Yangtze craton of China. *Precambrian Res.* **2006**, *146*, 16–34. [[CrossRef](#)]
8. Qiu, Y.; Gao, S.; McNaughton, N.J.; Ling, W. First evidence of >3.2 Ga continental crust in the Yangtze Craton of South China and its implications for Archean crustal evolution and Phanerozoic tectonics. *Geology* **2000**, *28*, 11–14. [[CrossRef](#)]
9. Gao, S.; Ling, W.; Qiu, Y.; McNaughton, N.J.; Groves, D.I. SHRIMP single zircon U–Pb dating of the Kongling high-grade metamorphic terrain: Evidence for >3.2 Ga old continental crust in the Yangtze craton. *Sci. China Earth Sci.* **2001**, *31*, 27–35, (In Chinese with English abstract).
10. Zheng, J.; Griffin, W.L.; O'Reilly, S.Y.; Zhang, M.; Pearson, N.; Pan, Y. Widespread Archean basement beneath the Yangtze craton. *Geology* **2006**, *34*, 417–420. [[CrossRef](#)]
11. Compston, W.; Williams, I.S.; Kirschvink, J.L.; Zhang, Z. Zircon U–Pb ages for the early Cambrian time-scale. *J. Geol. Soc.* **1992**, *149*, 171–184. [[CrossRef](#)]
12. Liu, H.; Xia, B.; Zhang, Y. Zircon SHRIMP dating of sodium alkaline rocks from Maomaogou area of Huili county in Panxi, SW China and its geological implications. *Chin. Sci. Bull.* **2004**, *49*, 1431–1438, (In Chinese with English abstract). [[CrossRef](#)]
13. Zhang, S.; Zheng, Y.; Wu, Y.; Zhao, Z.; Gao, S.; Wu, F. Zircon U–Pb age and Hf isotope evidence for 3.8 Ga crustal remnant and episodic reworking of Archean crust in South China. *Earth Planet. Sci. Lett.* **2006**, *252*, 56–71. [[CrossRef](#)]
14. Chen, Z.; Chen, S. *On the Tectonic Evolution of the West Margin of the Yangtze Block*; Chongqing Publishing House: Chongqing, China, 1987; pp. 1–172. (In Chinese)
15. Li, F.; Qin, J.; Shen, Y.; Yu, F.; Zhou, G.; Pan, X.; Li, X. *The Presinian in the Kangdian Area*; Chongqing Publishing House: Chongqing, China, 1988; pp. 1–453. (In Chinese)
16. Zhou, M.; Yan, D.; Kennedy, A.K.; Li, Y.; Ding, J. SHRIMP U–Pb zircon geochronological and geochemical evidence for Neoproterozoic arc-magmatism along the western margin of the Yangtze Block, South China. *Earth Planet. Sci. Lett.* **2002**, *196*, 51–67. [[CrossRef](#)]
17. Zhou, M.; Ma, Y.; Yan, D.; Xia, X.; Zhao, J.; Sun, M. The Yanbian Terrane (Southern Sichuan Province, SW China): A Neoproterozoic arc assemblage in the western margin of the Yangtze Block. *Precambrian Res.* **2006**, *144*, 19–38. [[CrossRef](#)]
18. Li, X.; Li, Z.; Ge, W.; Zhou, H.; Li, W.; Liu, Y.; Wingate, M.T.D. Neoproterozoic granitoids in South China: Crustal melting above a mantle plume at ca. 825 Ma? *Precambrian Res.* **2003**, *122*, 45–83. [[CrossRef](#)]
19. Geng, Y.; Yang, C.; Wang, X.; Ren, L.; Du, L.; Zhou, X. Age of Crystalline Basement in Western Margin of Yangtze Terrane. *Geol. J. China Univ.* **2007**, *13*, 429–441, (In Chinese with English abstract).
20. Lu, S.; Yang, C.; Li, H.; Chen, Z. North China continent and Columbia supercontinent. *Earth Sci. Front.* **2002**, *9*, 225–233, (In Chinese with English abstract).
21. Zhao, G.; Cawood, P.A.; Wilde, S.A.; Sun, M. A review of the global 2.1–1.8 Ga orogens: Implications for a pre-Rodinian supercontinent. *Earth Sci. Rev.* **2002**, *59*, 125–162. [[CrossRef](#)]
22. Zhao, X.; Zhou, M.; Li, J.; Sun, M.; Gao, J.; Sun, W.; Yang, J. Late Paleoproterozoic to Early Mesoproterozoic Dongchuan Group in Yunnan, SW China: Implications for tectonic evolution of the Yangtze Block. *Precambrian Res.* **2010**, *182*, 57–69. [[CrossRef](#)]
23. Zhao, G.; Li, S.; Sun, M.; Wilde, S.A. Assembly, accretion, and break-up of the Palaeo-Mesoproterozoic Columbia supercontinent: Record in the North China Craton revisited. *Int. Geol. Rev.* **2011**, *53*, 1331–1356. [[CrossRef](#)]
24. Zhao, G.; Cawood, P.A. Precambrian geology of China. *Precambrian Res.* **2012**, *222–223*, 13–54. [[CrossRef](#)]
25. Fan, H.; Zhu, W.; Li, Z.; Zhong, H.; Bai, Z.; He, D.; Chen, C.; Cao, C. Ca. 1.5 Ga mafic magmatism in south China during the break-up of the supercontinent Nuna/Columbia: The Zhuqing Fe–Ti–V oxide ore-bearing mafic intrusions in western Yangtze Block. *Lithos* **2013**, *168–169*, 85–98. [[CrossRef](#)]
26. Fan, H.; Zhu, W.; Chen, C. Review on Paleo-Mesoproterozoic strata and magmatic in the Kangdian area of the western margin of the Yangtze Block. *J. Earth Sci. Environ.* **2015**, *37*, 17–30, (In Chinese with English abstract).
27. Wang, D.; Yin, F.; Sun, Z.; Wang, L.; Wang, B.; Liao, S.; Tang, Y.; Ren, G. Zircon U–Pb age and Hf isotope of Paleoproterozoic mafic intrusion on the western margin of the Yangtze Block and their implications. *Geol. Bull. China* **2013**, *32*, 617–630, (In Chinese with English abstract).

28. Wang, W.; Zhou, M. Provenance and tectonic setting of the Paleo- to Mesoproterozoic Dongchuan Group in the southwestern Yangtze Block, South China: Implication for the breakup of the supercontinent. *Columbia Tectonophysics* **2014**, *610*, 110–127. [[CrossRef](#)]
29. Wang, W.; Zhou, M.; Zhao, X.; Chen, W.; Yan, D. Late paleoproterozoic to Mesoproterozoic rift successions in SW China: Implication for the Yangtze Block–North Australia–Northwest Laurentia connection in the Columbia supercontinent. *Sediment. Geol.* **2014**, *309*, 33–47. [[CrossRef](#)]
30. Zheng, Y.; Xiao, W.; Zhao, G. Introduction to tectonics of China. *Gondwana Res.* **2013**, *23*, 1189–1206. [[CrossRef](#)]
31. Zhu, W.; Bai, Z.; Hong, Z.; Ye, X.; Fan, H. The origin of the c. 1.7 Ga gabbroic intrusion in the Hekou area, SW China: Constraints from SIMS U–Pb zircon geochronology and elemental and Nd isotopic geochemistry. *Geol. Mag.* **2017**, *154*, 286–304. [[CrossRef](#)]
32. Qiu, X.; Yang, H.; Lu, S.; Tan, J.; Cai, Y. Geochronological and geochemical study for the Paleoproterozoic A-type granite in the nucleus of the Yangtze Craton and its tectonic implication. *Geoscience* **2015**, *29*, 884–895, (In Chinese with English abstract).
33. Deng, Q.; Wang, Z.; Wang, J.; Cui, X.; Ma, L.; Xiong, X. Discovery of the Baiyu ~1.79 Ga A-type Granite in the Beiba Area of the Northwestern Margin of Yangtze Block: Constraints on Tectonic Evolution of South China. *Acta Geol. Sin.* **2017**, *91*, 1454–1466, (In Chinese with English abstract).
34. Zhao, X.; Zhou, M. Fe–Cu deposits in the Kangdian region, SW China: A Proterozoic IOCG (ironoxide–copper–gold) metallogenic province. *Miner. Depos.* **2011**, *46*, 731–747. [[CrossRef](#)]
35. Guan, J.; Zheng, L.; Liu, J.; Sun, Z.; Cheng, W. Zircons SHRIMP U–Pb dating of diabase from Hekou, Sichuan Province, China and its geological significance. *Acta Geol. Sin.* **2011**, *85*, 482–490, (In Chinese with English abstract).
36. Guo, Y.; Wang, S.; Sun, X.; Wang, Z.; Yang, B.; Liao, Z.; Zhou, B.; Jiang, X.; Hou, L.; Yang, B. The Paleoproterozoic Breakup Event in the Southwest Yangtze Block: Evidence from U–Pb Zircon Age and Geochemistry of Diabase in Wuding, Yunnan Province, SW China. *Acta Geol. Sin.* **2014**, *88*, 1651–1665, (In Chinese with English abstract).
37. Wang, Z.; Guo, Y.; Yang, B.; Wang, S.; Sun, X.; Hou, L.; Zhou, B.; Liao, Z. Discovery of the 1.73 Ga Haizi anorogenic type granite in the western margin of Yangtze Craton, and its geological significance. *Acta Geol. Sin.* **2013**, *87*, 931–942, (In Chinese with English abstract).
38. Wang, S.; Liao, Z.; Sun, X.; Jiang, X.; Zhou, B.; Guo, Y.; Luo, M.; Zhu, H.; Ma, D. Geochemistry of Paleoproterozoic Diabases in the Dongchuan Copper Deposit, Yunnan, SW China: Response to Breakup of the Columbia Supercontinent in the Southwestern Margin of Yangtze Block. *Acta Geol. Sin.* **2013**, *87*, 1834–1852, (In Chinese with English abstract).
39. Wang, S.; Jiang, X.; Yang, B.; Sun, X.; Liao, Z.; Zhou, Q.; Guo, Y.; Wang, Z.; Yang, B. The Proterozoic Tectonic Movement in Kangdian Area I: Kunyang Intracontinental Rift, Mantle Plume and Its Metallogenesis. *Geol. Rev.* **2016**, *62*, 1353–1377.
40. Hou, L.; Ding, J.; Deng, J.; Peng, H. Geology, geochronology, and geochemistry of the Yinachang Fe–Cu–Au–Ree deposit of the Kangdian region of SW China: Evidence for a Paleo–Mesoproterozoic tectono-magmatic event and associated IOCG systems in the western Yangtze Block. *J. Asian Earth Sci.* **2015**, *103*, 129–149. [[CrossRef](#)]
41. Sun, Z.; Yin, F.; Guan, J.; Liu, J.; Li, J.; Geng, Q.; Wang, L. SHRIMP U–Pb dating and its stratigraphic significance of tuff zircons from Heishan Formation of Kunyang Group, Dongchuan area, Yunnan Province. *Geol. Bull. China* **2009**, *28*, 896–900, (In Chinese with English abstract).
42. Yin, F.; Sun, Z.; Ren, G.; Wang, D. Geological Record of Paleo- and Mesoproterozoic Orogenesis in the Western Margin of Upper Yangtze Block. *Acta Geol. Sin.* **2012**, *86*, 1917–1932, (In Chinese with English abstract).
43. Wang, D.; Sun, Z.; Yin, F.; Wang, L.; Wang, B.; Zhang, W. Geochronology of the Hekou Group on the western margin of the Yangtze Block: Evidence from zircon LA-ICP-MS U–Pb dating of volcanic rocks. *J. Stratigr.* **2012**, *36*, 630–635, (In Chinese with English abstract).
44. Yang, H.; Liu, P.; Meng, E.; Wang, F.; Xiao, L.; Liu, C. Geochemistry and its tectonic implications of metabasite in the Dahongshan Group in southwestern Yangtze block. *Acta Petrol. Sin.* **2014**, *30*, 3021–3033, (In Chinese with English abstract).

45. Zhu, Z.; Hou, K.; Zhu, K.; Tan, H. Geochronology and geochemistry of the Hekou Group in Sichuan Province, SW China. *Geochem. J.* **2013**, *47*, 51–64. [[CrossRef](#)]
46. Zhu, Z.; Tan, H.; Liu, Y. Late palaeoproterozoic Hekou Group in Sichuan, southwest China: Geochronological framework and tectonic implications. *Int. Geol. Rev.* **2018**, *60*, 305–318. [[CrossRef](#)]
47. Li, S.; Hart, S.R.; Zheng, S.; Liu, D.; Zhang, G.; Guo, A. Evidence of Sm–Nd isotopic ages in the collision period of North China and South China Land. *Chin. Sci. Ser. B* **1989**, *3*, 312–319. (In Chinese)
48. Li, S.; Jagoutz, E.; Chen, Y.; Li, Q. Sm–Nd and Rb–Sr isotopic chronology and cooling history of ultrahigh pressure metamorphic rocks and their country rocks at Shuanghe in the Dabie Mountains, Central China. *Geochim. Cosmochim. Acta* **2000**, *64*, 1077–1093. [[CrossRef](#)]
49. Li, Z.; Wartho, J.A.; Sandra, O.; Zhang, C.; Li, X.; Wang, J.; Bao, C. Early history of the eastern Sibao Orogen (South China) during the assembly of Rodinia: New mica $^{40}\text{Ar}/^{39}\text{Ar}$ dating and SHRIMP U–Pb detrital zircon provenance constraints. *Precambrian Res.* **2007**, *159*, 79–94. [[CrossRef](#)]
50. Dong, Y.; Liu, X.; Santosh, M.; Zhang, X.; Chen, Q.; Yang, C.; Yang, Z. Neoproterozoic subduction tectonics of the northwestern Yangtze Block in South China: Constrains from zircon U–Pb geochronology and geochemistry of mafic intrusions in the Hannan Massif. *Precambrian Res.* **2011**, *189*, 66–90. [[CrossRef](#)]
51. Liu, W.; Yang, X.; Ma, Z.; Sun, Z. Genesis of monzonitic granite in the northern margin of Yangtze Block: Zircon U–Pb chronology, Hf isotope and geochemical constraint. *Acta Geol. Sin.* **2018**, *92*, 65–76, (In Chinese with English abstract).
52. Xu, X.; Cheng, J.; Li, X.; Ma, Z.; Wang, H.; Li, P.; Li, T. Geochemical Constrains on the Petrogenesis and Tectonic Setting Discrimination of Volcanic Rocks from the Baimianxia and the Sanwan Formations. *Acta Geol. Sin.* **2009**, *83*, 1703–1718, (In Chinese with English abstract).
53. Xu, X.; Xia, L.; Chen, J.; Ma, Z.; Li, X.; Xia, Z.; Wang, H. Zircon U–Pb dating and geochemical study of volcanic rocks from Sunjiahe Formation of Xixiang Group in northern margin of Yangtze Plate. *Acta Petrol. Sin.* **2009**, *25*, 3309–3326, (In Chinese with English abstract).
54. Xu, X.; Chen, J.; Li, X.; Ma, Z.; Wang, H.; Xia, L.; Xia, Z.; Li, P.; Li, T. Geochemistry and petrogenesis of volcanic rocks from Sanlangpu Formation and Dashigou Formation. *Acta Petrol. Sin.* **2010**, *26*, 617–632, (In Chinese with English abstract).
55. Xu, X.; Li, T.; Chen, J.; Li, P.; Wang, H.; Li, Z. Zircon U–Pb age and petrogenesis of intrusions from Mengzi area in the northern margin of Yangtze plate. *Acta Petrol. Sin.* **2011**, *27*, 699–720, (In Chinese with English abstract).
56. Burchfiel, B.C.; Chen, Z.; Liu, Y.; Royden, L.H. Tectonics of the Longmen Shan and adjacent regions, Central China. *Int. Geol. Rev.* **1995**, *37*, 661–735. [[CrossRef](#)]
57. Chen, W.T.; Zhou, M.F.; Zhao, X.F. Late Paleoproterozoic sedimentary and mafic rocks in the Hekou area, SW china: Implication for the reconstruction of the Yangtze Block in Columbia. *Precambrian Res.* **2013**, *231*, 61–77. [[CrossRef](#)]
58. Zhao, J.; Zhou, M. Geochemistry of Neoproterozoic mafic intrusions in the Panzihua district (Sichuan Province, SW China): Implications for subduction-related metasomatism in the upper mantle. *Precambrian Res.* **2007**, *152*, 27–47. [[CrossRef](#)]
59. Li, Z.; Li, X.; Kinny, P.D.; Wang, J.; Zhang, S.; Zhou, H. Geochronology of Neoproterozoic syn-rift magmatism in the Yangtze Craton, South China and correlations with other continents. Evidence for a mantle superplume that broke up Rodinia. *Precambrian Res.* **2003**, *122*, 85–109. [[CrossRef](#)]
60. Mou, C.; Zhou, M. Meso-Proterozoic sedimentary facies and palaeogeographic framework of the Huili-Huidong region and its adjacent areas. *Tethyan Geol.* **1998**, *22*, 28–39.
61. Liu, Y.; Gao, S.; Hu, Z.; Gao, C.; Zong, K.; Wang, D. Continental and oceanic crust recycling-induced melt-peridotite interactions in the Trans-North China Orogen: U–Pb dating, Hf isotopes and trace elements in zircons of mantle xenoliths. *J. Petrol.* **2010**, *51*, 537–571. [[CrossRef](#)]
62. Wiedenbeck, M. An example of reverse discordance during ion microprobe zircon dating: An artifact of enhanced ion yields from a radiogenic labile Pb. *Chem. Geol.* **1995**, *125*, 197–218. [[CrossRef](#)]
63. Liu, Y.; Hu, Z.; Gao, S.; Günther, D.; Xu, J.; Gao, C.; Chen, H. In situ analysis of major and trace elements of anhydrous minerals by LA-ICP-MS without applying an internal standard. *Chem. Geol.* **2008**, *257*, 34–43. [[CrossRef](#)]
64. Ludwig, K.R. *A Geochronological Toolkit for Microsoft Excel*, Isoplot/Ex version 3.00; Berkeley Geochronology Center Special Publication: Berkeley, CA, USA, 2003; Volume 4, pp. 1–70.

65. Wu, F.; Yang, Y.; Xie, L.; Yang, J.; Xu, P. Hf isotopic compositions of the standard zircons and baddeleyites used in U–Pb geochronology. *Chem. Geol.* **2006**, *234*, 105–126. [[CrossRef](#)]
66. Black, L.P.; Kamo, S.L.; Williams, I.S.; Mundil, R.; Davis, D.W.; Korsch, R.J.; Foudoulis, C. The application of Shrimp to Phanerozoic geochronology; a critical appraisal of four zircon standards. *Chem. Geol.* **2003**, *200*, 171–188. [[CrossRef](#)]
67. Hoskin, P.W.O.; Black, L.P. Metamorphic zircon formation by solid-state recrystallization of protolith igneous zircon. *J. Metamorph. Geol.* **2000**, *18*, 423–443. [[CrossRef](#)]
68. Wu, Y.; Zheng, Y. Genesis of zircon and its constraints on interpretation of U–Pb age. *Chin. Sci. Bull.* **2004**, *49*, 1554–1569. [[CrossRef](#)]
69. Blichert-Toft, J.; Albarède, F. The isotope Lu–Hf geochemistry of the chondrites and the evolution of the mantle-crust system. *Earth Planet. Sci. Lett.* **1997**, *148*, 243–258. [[CrossRef](#)]
70. Griffin, W.L.; Pearson, N.J.; Belousova, E.; Jackson, S.E.; Achterbergh, E.V.; Suzanne, Y.; O'Reilly, S.Y.; Shee, S.R. The Hf isotope composition of cratonic mantle: LAM-MC-ICPMS analysis of zircon megacrysts in kimberlites. *Geochim. Cosmochim. Acta* **2000**, *64*, 133–147. [[CrossRef](#)]
71. Sano, Y.; Terada, K.; Hidaka, H.; Yokoyama, K.; Nutman, A.P. Alaeoproterozoic thermal events recorded in the ~4.0 Ga acasta gneiss, Canada: Evidence from shrimp U–Pb dating of apatite and zircon. *Geochim. Cosmochim. Acta* **1999**, *63*, 899–905. [[CrossRef](#)]
72. Wilde, S.A.; Valley, J.W.; Peck, W.H.; Graham, C.M. Evidence from detrital zircons for the existence of continental crust and oceans on the Earth 4.4 Ga ago. *Nature* **2001**, *409*, 175–178. [[CrossRef](#)] [[PubMed](#)]
73. Yang, J.; Gao, S.; Hu, Z.; Yuan, H.; Gong, H.; Li, M.; Xiao, G.; Wei, J. Age and growth of the Archean Kongling terrain, South China, with emphasis on 3.3 Ga granitoid gneisses. *Geochim. Cosmochim. Acta* **2008**, *72*, 153–182.
74. Jiao, W.; Wu, Y.; Yang, S.; Peng, M.; Wang, J. The oldest basement rock in the Yangtze craton revealed by zircon U–Pb age and Hf isotope composition. *Earth Sci. Ser. D* **2009**, *39*, 972–978, (In Chinese with English abstract). [[CrossRef](#)]
75. Wu, Y.; Gao, S.; Gong, H.; Xiang, H.; Jiao, W.; Yang, S.; Liu, Y.; Yuan, H. Zircon U–Pb age, trace Element and Hf isotope composition of Kongling terrane in the Yangtze Craton: Refining the timing of Palaeoproterozoic high-grade metamorphism. *J. Metamorph. Geol.* **2009**, *27*, 461–477. [[CrossRef](#)]
76. Wu, Y.; Chen, D.; Xia, Q.; Delouie, E.; Cheng, H. SIMS U–Pb dating of zircons in granulite of Huangtuling from northern Dabieshan. *Acta Petrol. Sin.* **2002**, *18*, 378–382, (In Chinese with English abstract).
77. Chavagnac, V.; Jahn, B.; Villa, I.M.; Whitehouse, M.J.; Liu, D. Multichronometric evidence for an in situ origin of the ultrahigh-pressure metamorphic terrane of Dabieshan, China. *J. Geol.* **2001**, *109*, 633–646. [[CrossRef](#)]
78. Chen, D.; Delouie, E.; Xia, Q.; Wu, Y.; Chen, H. Metamorphic zircon from Shuanghe ultra -high pressure eclogite, Dabieshan: Ion microprobe and internal micro-structure study. *Acta Petrol. Sin.* **2002**, *18*, 369–377, (In Chinese with English abstract).
79. Huang, J.; Zheng, Y.; Zhao, Z.; Wu, Y.; Zhou, J.; Liu, X. Melting of subducted continent: Element and isotopic evidence for a genetic relationship between Neoproterozoic and Mesozoic granitoids in the Sulu orogen. *Chem. Geol.* **2006**, *229*, 227–256. [[CrossRef](#)]
80. Chen, Y.; Luo, Z.; Zhao, J.; Li, Z.; Zhang, H.; Song, B. Petrogenesis and dating of the Kangding complex, Sichuan Province. *Earth Sci. Ser. D* **2004**, *34*, 687–697, (In Chinese with English abstract). [[CrossRef](#)]
81. Liu, X.; Gao, S.; Ling, W.; Yuan, H.; Hu, Z. Identification of 3.5 Ga detrital zircons from Yangtze Craton in South China and the implication for Archean crust evolution. *Prog. Nat. Sci.* **2005**, *15*, 1334–1337, (In Chinese with English abstract).
82. Zhang, X.; Zeng, Z.; Liu, W.; Pan, L.; Yang, B.; Liu, J.; Wei, Y.; He, C.; Li, S. Detrital zircon geochronology of Cambrian-Ordovician sedimentary rocks in southern Hunan-Northeast Guangxi area and its tectonic implications. *Geol. China* **2016**, *43*, 153–173, (In Chinese with English abstract).
83. Greentree, M.R.; Li, Z. The oldest known rocks in south-western China: SHRIMP U–Pb magmatic crystallisation age and detrital provenance analysis of the Paleoproterozoic Dahongshan Group. *J. Asian Earth Sci.* **2008**, *33*, 289–302. [[CrossRef](#)]
84. Yue, J.; Sun, X.; Trung, H.P.; Wang, P.; Tien, D.L.; Lang, Y.; Du, J. Pre-Cenozoic tectonic attribute and setting of the Song Da Zone, Vietnam. *Geotecton. Metallog.* **2013**, *37*, 261–570.

85. Lan, C.; Chung, S.; Lo, C.; Lee, T.; Wang, P.; Li, H.; van Toan, D. First evidence for Archean continental crust in northern Vietnam and its implications for crustal and tectonic evolution in Southeast Asia. *Gondwana Res.* **2001**, *29*, 219–222. [[CrossRef](#)]
86. Zhao, G.; Sun, M.; Wilde, S.A.; Li, S. Paleo-Mesoproterozoic supercontinent: Assembly, growth and breakup. *Earth Sci. Rev.* **2004**, *67*, 91–123. [[CrossRef](#)]
87. Hoffman, P.F. Speculations on Laurentia's first gigayear (2.0 to 1.0 Ga). *Geology* **1989**, *17*, 135–138. [[CrossRef](#)]
88. Santosh, M.; Zhao, D.; Kusky, T. Mantle dynamics of the Paleoproterozoic North China Craton: A perspective based on seismic tomography. *J. Geodyn.* **2010**, *49*, 39–53. [[CrossRef](#)]
89. Rogers, J.J.W.; Santosh, M. Tectonics and surface effects of the supercontinent Columbia. *Gondwana Res.* **2009**, *15*, 373–380. [[CrossRef](#)]
90. Zhang, S.; Zheng, Y.; Wu, Y.; Zhao, Z.; Gao, S.; Wu, F. Zircon U–Pb age and Hf–O isotope evidence for Paleoproterozoic metamorphic event in South China. *Precambrian Res.* **2006**, *151*, 265–288. [[CrossRef](#)]
91. Ling, W.; Gao, S.; Zhang, B.; Zhou, L.; Xu, Q. The recognizing of ca. 1.95 Ga tectono-thermal event in Kongling nucleus and its significance for the evolution of Yangtze Block, South China. *Sci. Bull.* **2001**, *45*, 2343–2348, (In Chinese with English abstract).
92. Yuan, H.; Zhang, Z.; Liu, W. Direct dating of zircon grains by $^{207}\text{Pb}/^{206}\text{Pb}$ ratio. *Miner. Petrol.* **1991**, *12*, 72–79, (In Chinese with English abstract).
93. Peng, M.; Wu, Y.; Wang, J.; Jiao, W. Paleoproterozoic mafic dyke from Kongling terrain in the Yangtze craton and its Implication. *Chin. Sci. Bull.* **2009**, *54*, 641–647, (In Chinese with English abstract). [[CrossRef](#)]
94. Wang, Z.; Wang, J.; Deng, Q.; Du, Q.; Zhou, X.; Yang, F.; Liu, H. Paleoproterozoic I-type granites and their implications for the Yangtze block position in the Columbia supercontinent: Evidence from the Lengshui Complex, South China. *Precambrian Res.* **2015**, *263*, 157–173. [[CrossRef](#)]
95. Eby, G.N. Chemical subdivision of the A-type granitoids: Petrogenetic and tectonic implications. *Geology* **1992**, *20*, 641–644. [[CrossRef](#)]



© 2018 by the authors. Licensee MDPI, Basel, Switzerland. This article is an open access article distributed under the terms and conditions of the Creative Commons Attribution (CC BY) license (<http://creativecommons.org/licenses/by/4.0/>).